Eur J Plant Pathol (2015) 143:237–260
DOI 10.1007/s10658-015-0677-9

Nitric oxide modulates redox-mediated defense in potato challenged with *Phytophthora infestans*

Dariusz Abramowski · Magdalena Arasimowicz-Jelonek · Karolina Izbiańska · Hanna Billert · Jolanta Floryszak-Wieczorek

Accepted: 6 May 2015 / Published online: 15 May 2015

Abstract In our experimental approach we investigated how post-infection nitric oxide-dependent signaling activated in potato leaves was related to defense against avirulent (avr) and virulent (vr) races of *Phytophthora infestans*. Results revealed that only in an incompatible response, early NO and superoxide ($O_2^{\bullet-}$) generation led to peroxynitrite ($ONOO^-$) formation and together with hydrogen peroxide (H_2O_2) production synchronized with SOD activity induced effective defense against *avr* pathogen. Early oxidative and nitrosative bursts triggered an imbalance in redox homeostasis in inoculated tissue. To counteract that effect, a total antioxidative capacity, ascorbate and sulfhydryl (-SH) group compounds increased both synergistically and markedly, confirming the precise mechanism of redox re-adjustment in *avr* oomycete -potato interaction. Moreover, the NO-coded message was stored and converted into an enhanced total SNO pool and particular S-nitrosylation of targeted proteins. Overall, we identified 104 proteins typed for S-nitrosylation in mock- or *P. infestans*-inoculated potato leaves. The S-nitrosoproteome structure comprised a wide repertoire of proteins, i.e. defense- and redox-related. Finally, only in the incompatible interaction, NO-based signal was rewritten on the rapid *PR-1* gene and PR-2 protein activation and was tuned with a limitation of late blight disease symptoms.

Keywords Reactive nitrogen species · Reactive oxygen species · Late blight · Biotin-switch · Redox homeostasis · Biotic stress

D. Abramowski (✉) · J. Floryszak-Wieczorek
Department of Plant Physiology, Poznan University of Life Sciences, Wolynska 35, 60 637 Poznan, Poland
e-mail: d.abram@up.poznan.pl

J. Floryszak-Wieczorek
e-mail: florysza@up.poznan.pl

M. Arasimowicz-Jelonek · K. Izbiańska
Department of Plant Ecophysiology, Adam Mickiewicz University, Umultowska 89, 61 614 Poznan, Poland

M. Arasimowicz-Jelonek
e-mail: marasimowicz@wp.pl

K. Izbiańska
e-mail: karolinaizbianska@wp.pl

H. Billert
Department of Experimental Anaesthesiology, Poznan University of Medical Sciences, Sw. Marii Magdaleny 14, 60 861 Poznan, Poland
e-mail: hbillert@ump.edu.pl

Introduction

During the evolutionary arms race, plants have developed many mechanisms to counteract the pathogen ingress and limit the severity of infection. Defense activation in plants is based on a complex signaling network orchestrated by reactive nitrogen (RNS) and oxygen species (ROS). Among them, nitric oxide (NO) as a free radical gas is a key player involved in diverse processes in plants, including response to multiple biotic and abiotic stress factors. A crucial role of NO in plant immune responses has been reported in different pathosystems including *Solanaceae* plants and

oomycete pathogens (Floryszak-Wieczorek et al. 2012; Janus et al. 2013). Noritake et al. (1996) reported for the first time the involvement of NO in potato innate immunity and demonstrated that pre-treatment of potato tubers with an NO donor (NOC-18) induced the accumulation of rishitin, an important phytoalexin in an establishment of constitutive resistance.

Moreover, the synchronized overproduction of NO and superoxide ($O_2^{\bullet-}$) in plants may lead to the formation of peroxynitrite ($ONOO^-$)—considered as an NO downstream signal and a potent modulator of the redox regulation in various cell signal transduction pathways. In contrast to animal system, where $ONOO^-$ executes cell death, in plants $ONOO^-$ is not indispensable in the activation of hypersensitive response (HR) (Delledonne et al. 2001). Hence, it is the co-operation of NO and active oxygen species, such as hydrogen peroxide (H_2O_2), induces HR in *Arabidopsis* after inoculation with *Pseudomonas syringae* pv. *maculicola* (*Psm*) or *tomato* (*Pst*) (Delledonne et al. 1998).

Efficient immune responses in plants are related to the early generation of highly reactive molecules with a high oxidizing potential, causing an imbalance in delicate redox homeostasis (Noctor et al. 2012). Therefore, restoration of cell balance by redox re-adjustment processes may somehow determine future adequate response (Groß et al. 2013). Maintaining the redox state by enzymatic and non-enzymatic apparatus in plants under stress conditions may eventually determine the efficiency of redox signaling in response to avr and vr pathogens, respectively.

Post-infection generation of NO may modify the total pool of S-nitrosothiols (SNOs) and convert NO-exported bioactivity into altered metabolism and *PR* gene expression (Astier et al. 2011). Interestingly, the NO-coded message may be stored in the post-translational modification of proteins. These, in turn, may be controlled by thioredoxins system and by trans-nitrosylation reactions with low-molecular mass thiols, governed mainly by GSNO reductase activity (Chaki and Lindermayr 2014).

Protein S-nitrosylation, based on NO equivalent transfer to cysteine thiol, is a reversible and redox-dependent modification regulating the activity of an increasing repertoire of proteins. The plant S-nitrosoproteome has been explored since 2005 and so far more than two hundred protein S-nitrosylation targets have been proposed (e.g. Lindermayr et al. 2005; Kato et al. 2013; Vanzo et al. 2014). Among them many await functional validation under control and stress conditions (Fares et al. 2014). In potato more than 80 proteins were found to undergo S-nitrosylation after exposure of potato leaves and tubers to S-nitrosoglutathione (Kato et al. 2013). In the presented paper, we used a modified biotin-switch technique to detect S-nitrosylation of proteins in mock- and *P. infestans*-inoculated potato leaves. Accumulating data suggest that storage of inactive signaling proteins and transcription factors may promote rapid immune response after de-nitrosylation and subsequent activation (Malik et al. 2011). Thus, deciphering the mechanism of NO-based signal storage and sensing on *PR* gene expression are pivotal in potato resistance to *P. infestans*.

In this study, we investigated how potato leaves exposed to avirulent and virulent *P. infestans* could activate post-stress NO signaling, moving towards or compromising resistance. For this purpose early and late interactions between reactive nitrogen and oxygen species were compared in the incompatible and compatible response. Thus, we provided evidence that NO-mediated changes re-written on protein S-nitrosylation were linked to redox homeostasis re-adjustment leading to PR protein accumulation and late blight disease control.

Materials and methods

Plant material and pathogen culture

A resistant potato line, *Solanum tuberosum* L. cv. 'Bzura' was derived from *in vitro* tissue culture and kept in sterile soil in a phytochamber (16 h/8 h : day/night; 180 μmol m^{-2} s^{-1}) at 18±1 °C and 60 % relative humidity up to the stage of eight leaves.

Pathogen culture and inoculation with *P. infestans*

Phytophthora infestans (Mont.) de Bary avirulent 1.3.4.7.10.11 (MP946) and virulent race 1.2.3.4.6.7.10 (MP977) were obtained from the Plant Breeding and Acclimatization Institute, Research Division at Młochów, Poland. Isolate MP946 in response to the used potato line triggered hypersensitive pointed cell death (HR) identified by us earlier as TUNEL-positive (Floryszak-Wieczorek et al. 2013). Potato plants were inoculated by spraying leaves with 5 ml of an oomycete zoospore suspension at a concentration of 1.0×10^5 per

1 ml of water and they were kept overnight at 100 % relative humidity and 18 °C and afterwards they were transferred to a growth chamber.

Assessment of disease index

The area under disease progress was assessed on potato leaves 7 days after inoculation with *P. infestans* and was based on a scale from I to IV (James 1971), which represented the percentage of leaf area covered by late blight symptoms (I=1 to 9 %; II=10 to 24 %; III=25 to 49 %; IV=50 to 100 %). Disease symptoms were also determined using trypan blue staining of *P. infestans* mycelium according to the assay proposed by Wilson and Coffey (1980), i.e. potato leaf discs (ø=2 cm) were inoculated with a zoospore suspension (40 μl). Imaging was performed by scanning leaf discs with a LIDE 210 Scanner (Canon). The blue stain corresponded to the area covered by *P. infestans* mycelium and was analyzed using the ImageJ 1.47v open source software (Wayne Raspand National Institutes of Health, USA).

Nitric oxide generation

The FL-NO fluorescence in extracts of potato leaves after inoculation was assayed spectrofluorimetrically using a selective nitric oxide sensor (CuFL) (Lim et al. 2006). The copper-complex of FL (2-{2-Chloro-6-hydroxy-5-[2-methylquinolin-8-ylamino)methyl]-3-oxo-3H-xanthen-9-l}benzoic acid) was prepared as 1 mM water stock solution according to the manufacturer's instructions (Strem Chemicals). Leaf tissue (500 mg of fresh weight) was homogenized in 2 ml of 10 mM potassium-phosphate buffer (pH 6.0). The extract was centrifuged at 21,000×g for 30 min at 4 °C. Then, 100 μl of supernatant were immediately used for NO assay by adding CuFL to the final concentration of 2 μM. Fluorescence intensity was determined with the Fluorescence Spectrometer Perkin Elmer LS 50B (UK) using 488 and 516 nm for excitation and emission, respectively. Each value was expressed as relative fluorescence intensity [Int×g^{-1} FW].

Superoxide radical production

Superoxide accumulation was determined by monitoring the reduction of NBT to diformazan in the presence of $O_2^{\bullet-}$ according to Doke (1983). The amount of reduced NBT was measured at a wavelength of 580 nm. The reference sample consisted of the incubation mixture lacking plant material. The $O_2^{\bullet-}$ level was expressed as ΔA_{580} [$h^{-1}\times g^{-1}$ FW].

Peroxynitrite formation

The level of peroxynitrite was assayed according to Huang et al. (2007) using folic acid as the peroxynitrite scavenger, giving a high fluorescent emission product. Fluorescence intensity of the solution was recorded at 460 nm with the excitation wavelength set at 380 nm. The standard curve was prepared for SIN-1 (Sigma-Aldrich) as a donor of peroxynitrite.

Hydrogen peroxide accumulation

The concentration of H_2O_2 was assayed spectrophotometrically using a titanium (Ti^{4+}) method described by Becana et al. (1986). Fresh leaves (0.25 g) were homogenized in 3 ml of 0.1 M potassium phosphate buffer (pH 7.8). After centrifugation (15,000×g for 30 min), the supernatant was used for further assays. The reaction mixture (1.5 ml) contained 0.1 M potassium-phosphate buffer (pH 7.8), enzymatic extract (400 μl) and titanium reagent. Titanium reagent was prepared on the day of assay by mixing 0.6 mM solution of 4-(2-pyridylazo) resorcinol and 0.6 mM potassium titanium tartrate at a 1:1 ratio. The concentration of H_2O_2 was determined by measuring absorbance at a wavelength of 508 nm against a calibration curve and expressed as μmol $H_2O_2\times g^{-1}$ FW.

S-nitrosothiol total pool quantification

Total SNO content was determined by chemiluminescence using a Sievers® Nitric Oxide Analyzer NOA 280i (GE Analytical Instruments, USA) according to the procedure proposed by Chaki et al. (2009). The detection of SNOs was based on reductive decomposition of nitroso compounds by an iodine/triiodide mixture in the presence of copper and conducted under red safety light. Fresh leaves (0.250 g) were homogenized in Tris–HCl 0.1 M buffer pH 7.5 (1:4, w/v) containing 100 μM DTPA, 1 mM EDTA, 1 mM EGTA, 1 mM PMSF, 0.1 mM neocuproine, 3.5 % (w/v) PVPP, 0.25 % (v/v) Triton X-100 and centrifuged at 3,000×g for 10 min. The supernatants were incubated with 10 mM NEM (N-ethylmaleimide) for 15 min at 4 °C and subsequently two aliquots were prepared for each sample.

To remove nitrite one aliquot was incubated for 15 min with 10 mM sulphanilamide at 4 °C. To eliminate nitrite and decompose SNOs the next aliquot was treated with 10 mM sulphanilamide and 7.3 mM $HgCl_2$ for 15 min at 4 °C. The difference between detected signals obtained from these aliquots demonstrated the total SNO content.

Total sulfhydryl group content

The status of -SH groups was assayed spectrophotometrically according to Rice-Evans et al. (1991). Fresh leaves (250 mg) were homogenized in 2 ml of 0.1 m citrate buffer (pH 3.0). After centrifugation at 15,000×g for 15 min, 300 μl of supernatant were collected and 10 % sodium dodecyl sulfate (SDS) and 10 mM sodium-phosphate buffer (pH 8.0) were added. Initial absorbance (A_0) was measured after mixing at a wavelength of 412 nm. Next, 5,5′-dithiobis-(2-nitrobenzoic acid) (DTNB) was added and the mixture was incubated for 1 h at 37 °C. Simultaneously, the control sample was prepared with 10 mM sodium-phosphate buffer (pH 8.0) instead of DTNB. Final absorbance (A_1) was measured at a wavelength of 412 nm. The difference in absorbance A_1-A_0 (after subtracting an analogous value obtained for the control sample) was a measure of –SH group content in the sample. Sulfhydryl group content was expressed as glutathione equivalents [μmol GSH×g^{-1} FW].

Ascorbate level

For the determination of ascorbate the spectrophotometric assay was used as described by Mukherjee and Choudhuri (1983). Fresh leaves (250 mg) were homogenized in 5 % triacetic acid (TCA) (1:8; w/v) and then centrifuged at 15,000×g for 20 min at 4 °C. To TCA-diluted supernatant 10 μl of 10 % thiourea and 500 μl of 0.28 % dinitrophenyl hydrazine in 1 M HCl (w/v) were added. After 20 min incubation at 100 °C and cooling on ice bath, 1.25 ml 80 % H_2SO_4 was added to stop the reaction. Absorbance was measured at 530 nm and obtained results were calculated according to the standard curve in the range 1–12 μg ml^{-1} ascorbate.

Total antioxidantive capacity

Total antioxidative capacity was based on leaf extract capacity to reduce the 2,2′-azinobis-(3-ethylbenzothiazoline-6-sulfonic acid) (ABTS) cation radical according to the method proposed by Re et al. (1999). Initial $ABTS^+$ solution was diluted with 0.1 M potassium-phosphate buffer (pH 7.4) to set absorbance at a wavelength of 414 nm on 1.0. Fresh leaves (250 mg) were homogenized in 2 ml of 5 % TCA and centrifuged at 15,000×g for 15 min. The volume of 980 μl diluted $ABTS^+$ was pipetted to a cuvette and absorbance (A_0) was measured at a wavelength of 414 nm. Next, 20 μl of the extract were added and absorbance was measured again after 10 s (A_2) and 30 min (A_1), respectively. Fast antioxidants were calculated as $\Delta A_{fast}=A_1-A_0$. Slow antioxidants were calculated as $\Delta A_{slow}=(A_2-A_1)-(A_2'-A_1')$. The calibration curve was prepared by successively adding 5 μl portions of 0.01 mM Trolox® to $ABTS^+$ and measuring a decrease of absorbance. The final result of total antioxidative capacity was expressed in mM Trolox×g^{-1} FW.

Enzyme activities

NADPH oxidase [EC 1.6.3.1]

The NADPH dependent $O_2^{\bullet-}$ generating activity was determined by a modified assay based on a reduction of XTT by $O_2^{\bullet-}$ anions according to the method of Able et al. (1998). Fresh leaves (0.5 g) were homogenized in 50 mM potassium-phosphate buffer, pH 7.0 (1:4; w/v), containing 0.1 % Triton X-100 (v/v), 1 % PVP, 0.04 % Na_2O_5, 1 mM EDTA and centrifuged at 18,000×g for 20 min. Supernatants were passed through Sephadex G-25 gel filtration columns (Illustra NAP-10, GE Healthcare) and served as the enzyme extract. The volume of 1 ml assay reaction mixture contained 0.5 mM XTT, 0.1 mM NADPH and 30 μl enzyme extract in 50 mM Tris–HCl buffer, pH 7.5. XTT reduction was determined at 470 nm and rates of $O_2^{\bullet-}$ generation were calculated using an extinction coefficient for XTT of 2.16×10^4 M^{-1} cm^{-1} and the enzyme activity was expressed as μmol $O_2^{\bullet-}$×min^{-1}×mg^{-1} protein.

Superoxide dismutase [EC 1.15.1.1.]

SOD activity was assayed by measuring SOD ability to inhibit the photochemical reduction of NBT using the method of Beauchamp and Fridovich (1971). Fresh leaves (250 mg) were homogenized in 0.05 M potassium-phosphate buffer, pH 7.0 (1:12; w/v), containing 1 % PVPP, 1 mM EDTA, 0.01 M NaCl and centrifuged at 20,000×g for 30 min. The assay mixture contained 0.05 M sodium phosphate buffer (pH 7.8),

13 mM methionine, 75 μM NBT, enzymatic extract and 2 μM of riboflavin. The reaction was initiated by UV radiation (15 W) and was run for 15 min. The absorbance was measured at a wavelength of 560 nm. The amount of enzyme that caused inhibition of the NTB reduction reaction by 50 % was assumed as a unit of SOD activity ($U \times mg^{-1}$ protein).

S-nitrosoglutathione reductase [EC 1.2.1.46]

The GSNOR activity was determined according to the procedure proposed by Barroso et al. (2006) with minor modifications. Fresh leaves (500 mg) were homogenized in 0.1 M Tris–HCl buffer, pH 7.5 (1:4 w/v) containing 0.2 % Triton X-100 (v/v), 10 % glycerol (v/v), 0.1 mM EDTA, 2 mM DTT at 4 °C and centrifuged at 27,000×g for 25 min. The supernatant was passed through Sephadex G-25 gel filtration columns (Illustra NAP-10, GE Healthcare), then immediately through Amicon Ultra 3 K Filters (Millipore) and served as the enzyme extract. The assay reaction mixture of 1 ml contained 0.5 mM EDTA, 0.2 mM NADH, 0.4 mM GSNO and 30 μl enzyme extract in 25 mM Tris–HCl buffer, pH 8.0. The reaction was held at 25 °C and initiated with an addition of GSNO (Sigma Aldrich). NADH oxidation was determined at 340 nm and rates of NADH consumed at min^{-1} were calculated using an extinction coefficient of 6220 $M^{-1} \times cm^{-1}$.

β-1,3-glucanase [EC 3.2.1.6]

The β-1,3-glucanse (PR-2) activity was determined according to the procedure proposed by Abeles and Forrence (1970) in a colorimetric assay utilizing laminarin as a substrate. Fresh leaves (250 mg) were homogenized in 0.05 M potassium-acetate buffer, pH 5.0 (1:16; w/v), containing 0.125 g Polyclar AT and then centrifuged at 15,000×g for 25 min. The supernatant (0.5 ml) was added to 0.5 ml 2 % (w/v) laminarin aqueous solution and was incubated for 2 h at 50 °C. After stopping the reaction and dilution (1 : 10), optical density was read at 500 nm. The β-1,3-glucanase activity was determined as the level of reducing sugars produced and served as glucose equivalents [μmol glucose× $min^{-1} \times mg^{-1}$ protein]; finally PR-2 activity was expressed as % of control.

Chitinase [EC 3.2.1.14]

The chitinase (PR-3) activity was determined in a colorimetric assay utilizing CM–Chitin–RVB (LOEWE Biochemica) as a substrate (Pauly et al. 1999). Fresh leaves (250 mg) were homogenized in 0.05 M potassium-acetate buffer, pH 5.0 (1:16; w/v), and then centrifuged at 10,000×g for 10 min. The volume of 0.2 ml of the enzymatic fraction was added to 0.2 ml CM–Chitin–RVB ($2\ mg \times ml^{-1}$) and 0.4 ml of homogenization buffer. Then the reaction mixture was incubated for 1 h at 37 °C and stopped by adding 0.2 ml 2 M HCl. The reaction mixture was centrifuged at 10,000×g for 5 min and the supernatant was collected to measure optical density at 550 nm. Chitinase activity was calculated according to the standard curve prepared with the use of recombinant *Streptomyces griseus* chitinase at 0.005–0.130 mU (Sigma-Aldrich). Enzyme activity was expressed as % of control.

Gene expression measurement

The RNA was isolated from 150 mg of frozen leaf using TriReagent® (Sigma) according to the method of Chomczynski and Sacchi (1987). The obtained RNA was purified with the use of a Deoxyribonuclease I Kit (Sigma). For the reverse transcription 1 μl of RNA from every experimental variant was processed with a RevertAid™ Reverse Transcriptase Kit (Thermo Scientific) according to the manufacturer's instructions. Real-time PCR was performed on a Rotor Gene 6000 Thermocycler (Corbett Life Sciences). The reaction mixture contained 0.1 μM of each primer, 1 μl of 5× diluted cDNA, 10 μl of the Power SYBR® Green PCR Master mix (Applied Biosystems) and DEPC-treated water to the total volume of 20 μl. The real-time PCR reaction conditions included an initial 5-min denaturation at 95 °C, followed by 55 cycles consisting of 10 s at 95 °C, 20 s at 53 °C and 30 s at 72 °C. The reaction was finalized by denaturation at a temperature rising from 72 to 95 °C by one degree at every 5 s. Reaction specificity was confirmed by the occurrence of one peak in the melting curve analysis. PR-1 primers used in real-time detection were as follows:

F: CCGCGTTGAGCTGGGGGAAA, R: GAGCTG GGGACTGCAGGATGC (T_m=53 °C). The data were normalized to the reference gene encoding elongation factor (ef1α, AB061263; F: ATTGGAAACGGATATG CTCCA, R: TCCTTACCTGAACGCCTGTCA, T_m=

53 °C). All used primers were designed using Primer-BLAST (Ye et al. 2012). The C_t values were determined with the use of a Real-time PCR Miner (Zhao and Fernald 2005) and the relative gene expression was calculated with the use of efficiency corrected calculation models presented by Pfaffl (2001).

Detection of endogenously S-nitrosylated proteins in potato leaves by the modified biotin-switch technique

The *in vivo* S-nitrosylated proteins were detected with the use of the modified biotin-switch technique (Lindermayr et al. 2005; Vanzo et al. 2014). Briefly, 250 mg of frozen leaf powder was mixed with 1 ml of HENT buffer containing 100 mM HEPES-NaOH pH 7.4, 10 mM EDTA, 0.1 mM neocuproine and 1 % (v/v) Triton X-100. After 15 min incubation the mixture was centrifuged at 4 °C for 10 min at 12,000×g. Protein concentration was measured using Bradford reagent and was adjusted to 1 μg×μl of HEN buffer, containing cOmplete™ protease inhibitor cocktail tablets (Roche). The blocking step was performed with the use of four volumes of freshly prepared HENS buffer (225 mM HEPES-NaOH pH 7.2, 0.9 mM EDTA, 0.1 mM Neocuproine, 2.5 % (w/v) SDS) and 30 mM NEM. Then the extracts were incubated at 37 °C for 30 min. After incubation excess blocking agent was removed by ice-cold acetone precipitation. The pellet was re-suspended in 0.1 ml HENS buffer (without NEM) per 1 mg of protein. Reduction of –SNOs and simultaneous biotinylation were performed using 1 mM biotin-HPDP (EZ-LinkTM Biotin-HPDP; Thermo scientific) and 3 mM reductant sinapinic acid (Sigma-Aldrich) for 1 h at 25 °C in darkness. Next, the precipitation using ice-cold acetone was conducted and the obtained pellets were re-suspended in non-reducing sample buffer and subjected to electrophoresis and Western blot analysis. Series of controls were performed including the positive signal control (omitting the blocking step) and the false-positive signal (omitting the biotinylation step). Electrophoresis was performed in non-reducing SDS-PAGE on gradient 4-20 % polyacrylamide gels (Mini-PROTEAN® Precast Gels, Biorad) followed by electrotransfer to the PFDF membrane (Millipore). The membrane was blocked using 1 % bovine serum albumin for 1 h, and the blots were then incubated with the anti-biotin mouse monoclonal antibody conjugated with alkaline-phosphatase (dilution 1:25000; Sigma-Aldrich) for 24 h. Further, the protein bands were visualized using 5-bromo-4-chloro-3-indolyl phosphate and nitro blue tetrazolium (SigmaFast BCIP, Sigma-Aldrich) according to the manufacturer's instructions.

Identification of proteins using mass spectrometry

Identification and analyses of proteins were performed with the use of a liquid chromatograph coupled with a mass spectrometer at the Mass Spectrometry Laboratory, the Institute of Biochemistry and Biophysics, the Polish Academy of Sciences. Protein bands were excised from the PVDF membrane and placed in 100 mM ammonium carbonate (pH 8.0) and directly subjected to the digestion procedure (overnight with 10 $ng \times \mu l^{-1}$ trypsin). After simultaneous reduction with 10 mM DTT (30 min at 56 °C) and alkylation with iodoacetamide (in darkness for 45 min at room temperature) the resulting peptide mixtures were concentrated and desalted on a RP-C18 pre-column (Waters). Further peptide separation was run on a nano- Ultra Performance Liquid Chromatography (UPLC) RP-C18 column (Waters, BEH130 C18 column, 75 μm i.d., 250 mm long) of a nanoACQUITY UPLC system, using a 45-min linear acetonitrile gradient. The column outlet was directly coupled to the Electrospray ionization (ESI) ion source of the Orbitrap Velos type mass spectrometer (Thermo), working in the regime of data dependent on the MS to MS/MS switch with HCD type peptide fragmentation. An electrospray voltage of 1.5 kV was used. Raw data files were pre-processed with the Mascot Distiller software (version 2.4.2.0, MatrixScience). The obtained peptide masses and fragmentation spectra were matched to the National Center Biotechnology Information (NCBI) non-redundant database (37425594 sequences; 13257553858 residues) with a *Viridiplantae* filter (1760563 sequences) using the Mascot search engine (Mascot Daemon v. 2.4.0, Mascot Server v. 2.4.1, MatrixScience). The following search parameters were applied: enzyme specificity was set to semiTrypsin, peptide mass tolerance to±30 ppm and fragment mass tolerance to±0.1 Da. The protein mass was left unrestricted, while mass values were set as monoisotopic with two missed cleavages being allowed. Alkylation of cysteine by carbamidomethylation, oxidation of methionine and carboxymethylation on lysine were set as a variable modification.

Statistical analysis

All results were based on at least three independent experiments, each with at least three biological replicates. Analysis of variance was conducted and the least significant differences (LSD) between means were determined using Tukey's test at a level of significance $P = 0.05$. SigmaPlot 11.0 (Systat) was used to perform statistical tests. Randomization was performed during collection of samples in histochemical assay of trypan blue staining.

Results

Generation of reactive nitrogen and oxygen species in potato leaves exposed to *P. infestans*

Semi-quantitative measurement of NO generation in potato leaves after inoculation was performed using the NO-selective fluorescent probe copper-complex of FL (Cu-FL). The avirulent race triggered an enhanced NO generation in potato leaves early after inoculation, with the maximum overproduction at 3 hpi (Fig. 1a). In contrast, virulent *P. infestans* provoked minor changes in the NO status similar to that of the mock-inoculated leaves. Augmented NO synthesis in *avr P. infestans*-inoculated potato was accompanied by enhanced $O_2^{\bullet-}$ generation (Fig. 1b). Both races of the pathogen caused a sustained increase of the $O_2^{\bullet-}$ level with the similar kinetics. Synchronized generations of NO and $O_2^{\bullet-}$ in the *avr P. infestans*-potato system increased the formation of peroxynitrite ($ONOO^-$) at 3 hpi (Fig. 1c). In turn, in the compatible interaction the kinetics of $ONOO^-$ formation showed a late accumulation at 24 hpi (Fig. 1c). Boosted generation of $O_2^{\bullet-}$ could be a result of controlled $O_2^{\bullet-}$ synthesis by NADPH oxidase. Hence, in the incompatible interaction the activity of NADPH oxidase was strongly induced from 1 hpi, reaching a two-fold increase in relation to uninoculated leaves (Fig. 1d). In the compatible interaction an up-regulation of NADPH oxidase was recorded later from 3 hpi (Fig. 1d). It was also found that *avr P. infestans* caused a considerably enhanced H_2O_2 overproduction in each tested time-point after inoculation (Fig. 1e), whereas in the compatible interaction only moderate changes were recorded. Moreover, in the incompatible interaction the above-mentioned changes in H_2O_2 content correlated in the time-dependent manner with the activity of superoxide dismutase (SOD). SOD was significantly up-regulated throughout the whole analyzed 24-h-period, reaching a steady two-times higher level in relation to healthy leaves (Fig. 1f).

Metabolic status of NO in potato leaves after inoculation

To gain further insight into NO-dependent down-stream signaling in potato, the S-nitrosothiols (SNOs) total pool was analyzed using precise chemiluminescence assay. An increased storage of the NO message in the total SNOs content was observed in *avr P. infestans*-treated potato from 1 hpi, attaining the highest level at 24 hpi (Fig. 2a). In contrast, the SNO pool remained unchanged in potato inoculated with the virulent race of the pathogen. The SNO level is prone to be regulated by GSNO reductase, capable of GSNO turn-over and affecting trans-nitrosylation processes. GSNOR activity was only moderately down-regulated in *avr P. infestans*-inoculated leaves (Fig. 2b). However, it must be stated that a lack of strong time-dependent correlation was found between GSNOR activity and the SNO pool. Furthermore, the complex management of NO-initiated pathway involves changes in S-nitrosoproteome structure. By performing the modified biotin-switch assay coupled to quantitative LC-MS/MS analysis, 104 protein targets of S-nitrosylation in potato were proposed. Supplementary Table 1 presents a list of *in vivo* S-nitrosylated proteins in mock- and *P. infestans*-treated potato leaves. Proteins typed for S-nitrosylation were clustered into 5 main functional groups (Fig. 6d Appendix). The most abundant cluster of 'metabolic enzymes' involved 44 % of the identified S-nitrosoproteome. 'Photosynthesis-involved proteins' comprising proteins orchestrating photosynthetic light reactions and the Calvin-Benson cycle were the second most intensely represented (24 %). The following less frequent groups included 'redox-related proteins' and 'defense-related proteins' each representing 6 % of the total number of modified proteins, respectively. Approx. 60 % of identified S-nitrosylation candidates have not been presented so far as potential members of the S-nitrosoproteome in plants and only 17 of them were reported earlier as S-nitrosylation targets in potato leaves and tubers supplied with GSNO (Kato et al. 2013). Since S-nitrosylation is under strong control of redox status of the cell, antioxidative enzymatic and non-enzymatic changes have been recorded upon *P. infestans* inoculation.

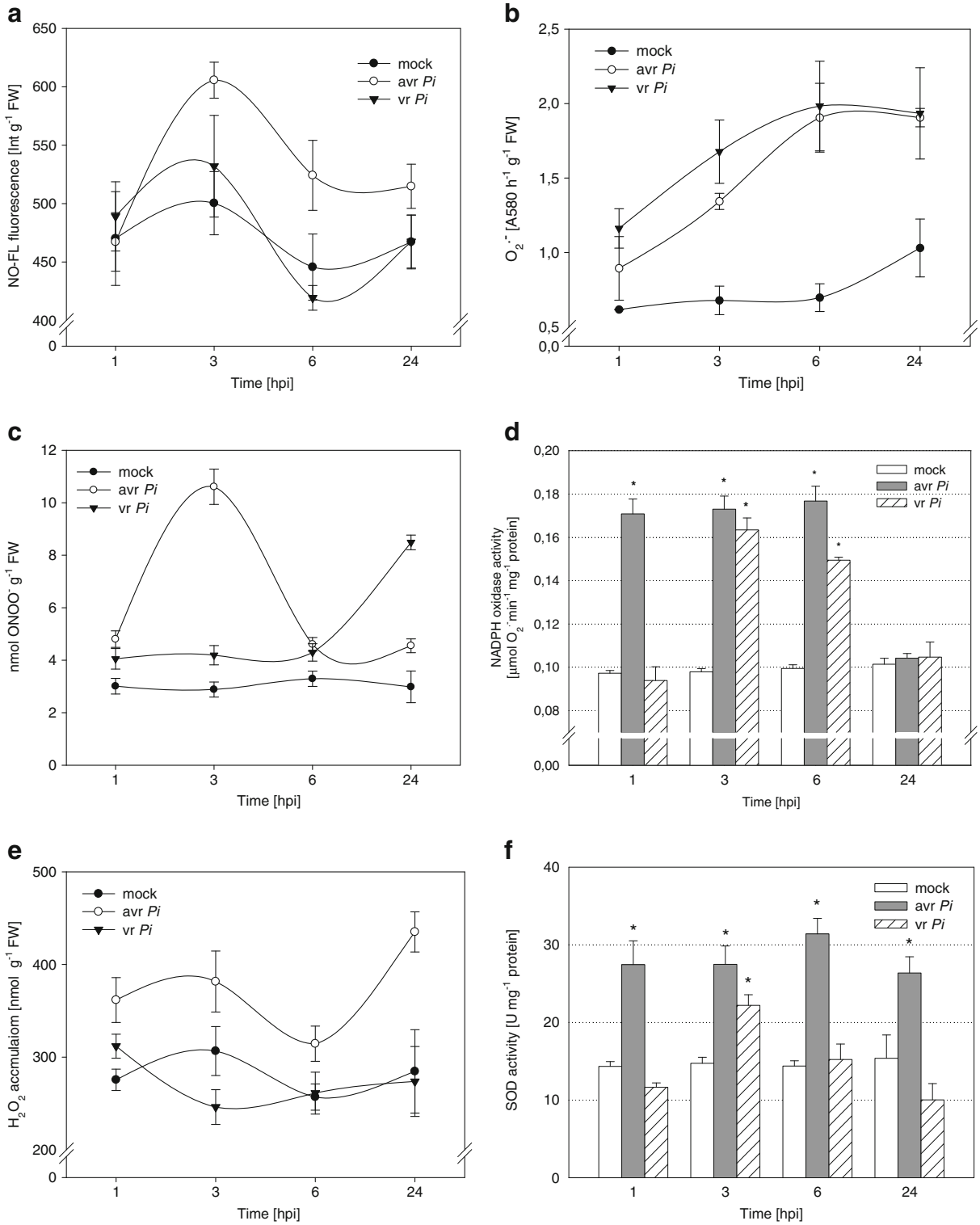

Fig. 1 The effect of *P. infestans* inoculation on potato leaves cv. 'Bzura': **a** nitric oxide (NO) and **b** superoxide radical ($O_2^{\bullet-}$) generation, **c** formation of peroxynitrite ($ONOO^-$), **d** activity of NADPH oxidase (NOX), **e** accumulation of hydrogen peroxide (H_2O_2), **f** activity of superoxide dismutase (SOD), * significantly different from mock-inoculated potato leaves, $P<0.05$. Values represent the average of data±SD of three independent experiments

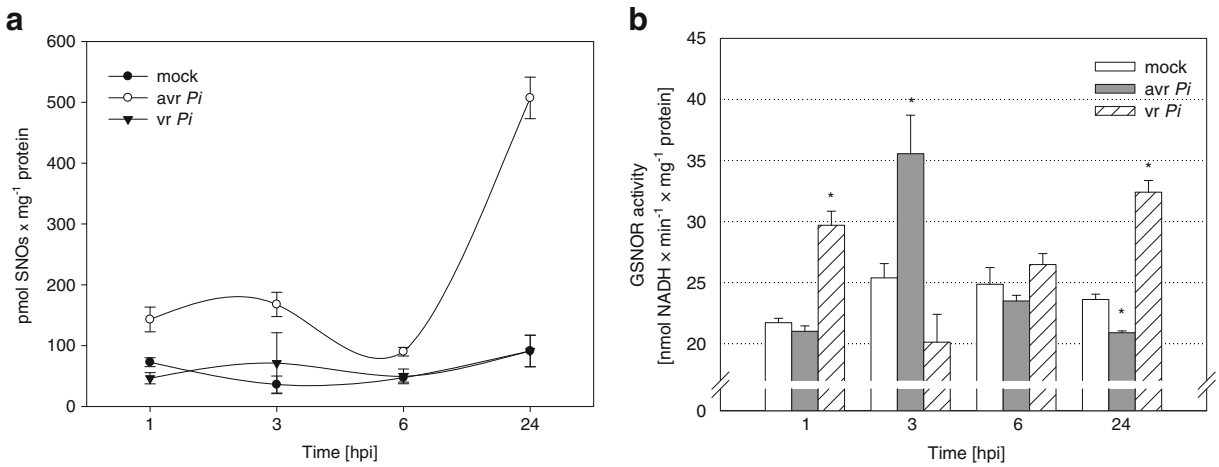

Fig. 2 The effect of *P. infestans* inoculation on potato leaves cv. 'Bzura': **a** activity of GSNO reductase (GSNOR), **b** total content of S-nitrosothiols (SNOs) determined by chemiluminescence assay using Sievers® Nitric Oxide Analyzer NOA 280i, * significantly different from mock-inoculated potato leaves, $P<0.05$. Values represent the average of data±SD of three independent experiments

Redox balance in inoculated leaves

Pathogens could trigger an imbalance in redox homeostasis in host-plant cells to maximize the opportunity of colonization. Therefore, selected non-enzymatic and enzymatic components of the redox maintenance apparatus were analyzed in potato leaves. In the incompatible interaction with *P. infestans* the total content of free sulfhydryl groups (-SH) (Fig. 3a) and ascorbate (Fig. 3b) increased notably at the early phase (1-3 hpi). It reached an approximately 2-fold and 3-fold higher concentration in relation to mock-inoculated and *vr P. infestans*-treated leaves, respectively. The early shift into the reductive potential was also confirmed by the expanded total antioxidative capacity referred to both the slow (Fig. 3c) and the fast (Fig. 3d) antioxidants. Thus, non-enzymatic components of the redox apparatus had a significant impact on the redox state re-adjustment towards the reductive potential in potato after ROS and RNS generation (Fig. 1a, b, c).

Pathogenesis-related protein up-regulation and disease progress

Late blight disease spots developed mainly after colonization with the virulent race of *P. infestans*. Severe foliar damage was observed in more than 75 % of leaves at 7 dpi (Fig. 4d) and the oomycete mycelium covered more than 20 % of leaf discs at 5 dpi (Fig. 5 Appendix). In *avr P. infestans*-treated leaves disease spots were smaller than 3 % of total area. The reduced disease symptoms corresponded to the enhanced defense responses in *avr P. infestans*-inoculated potato. Semi-quantitative real time RT-PCR revealed that *PR-1* gene expression was rapidly activated upon inoculation with *avr P. infestans* at the early phase (10-fold increase) and the mRNA level remained multiplied till 24 hpi (Fig. 4a). In the compatible interaction the robust *PR-1* gene transcript accumulation was recorded solely at the late phase at 24 hpi. However, the *PR-1* mRNA level raised gradually since 3 hpi. The indication of *PR-1* gene was accompanied by an effectively up-regulated β-1,3-glucanase activity (PR-2) (Fig. 4b). A less intense activation of PR-2 was found in the compatible interaction after pathogen ingress. In turn, chitinase (PR-3) activity was induced with a distinct magnitude at 3 hpi in both interactions (Fig. 4c), showing slight contributions to the effective defense against oomycete pathogens. The comparison of spatiotemporal *PR-1* and PR-2 analyses revealed stronger induction of the aforementioned PRs in response to the avirulent rather than the virulent race of *P. infestans*.

Discussion

In order to gain further insight into the NO-mediated multilevel interaction leading to potato immune

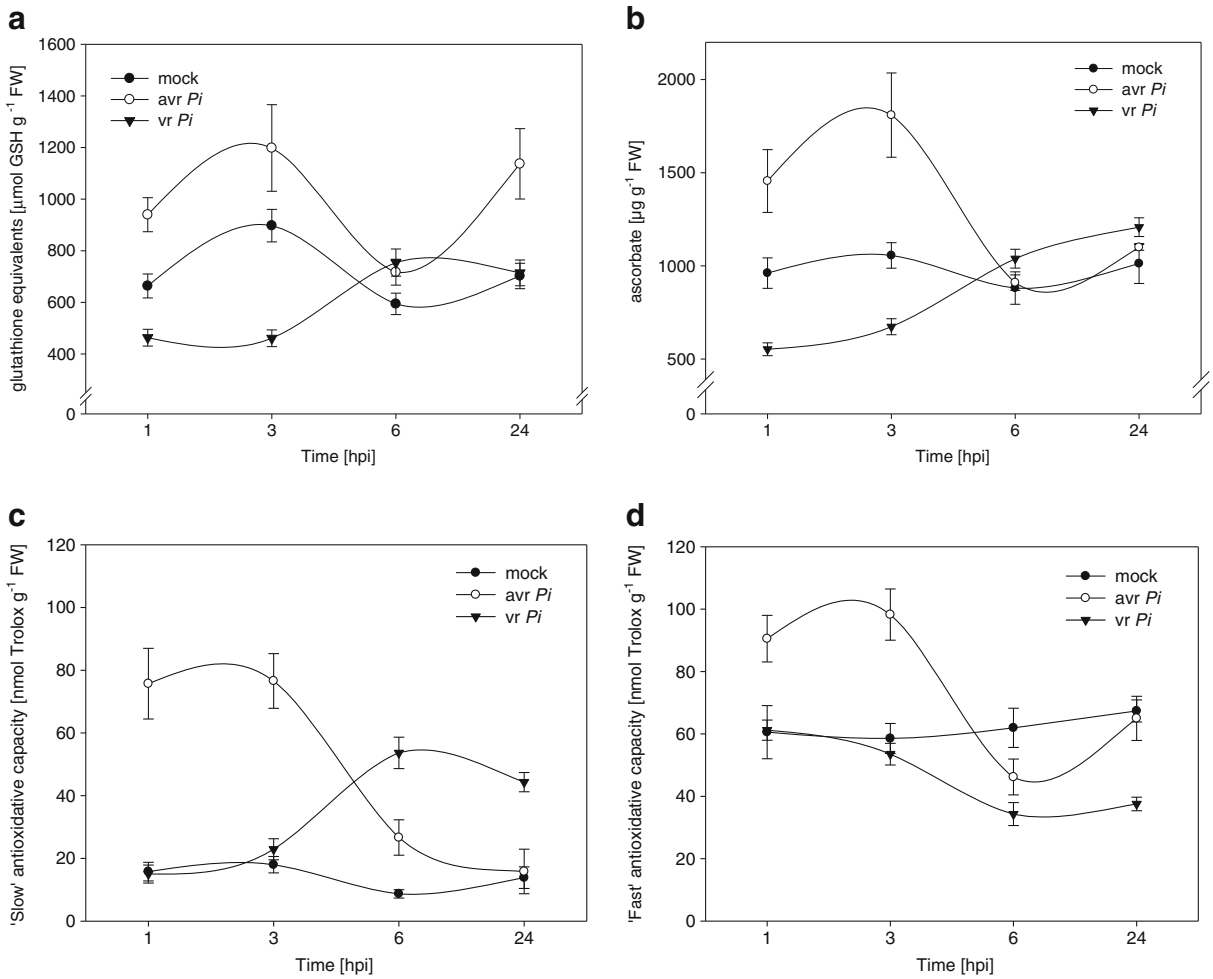

Fig. 3 The effect of *P. infestans* inoculation on redox state readjustments in potato leaves cv. 'Bzura': **a** total sulfhydryl (–SH) group content, **b** ascorbate concentration, **c** slow and **d** fast antioxidants referred to as total antioxidant capacity, * significantly different from mock-inoculated potato leaves, $P<0.05$. Values represent the average of data±SD of three independent experiments

response, two *P. infestans* races were used to induce the incompatible and compatible interaction, respectively. The activated defense signaling network was potentially NO-initiated and ranged from the S-nitrosylation of proteins to the execution of PR proteins storage. To date, NO functions in plants are far from being fully described. However, much progress has been achieved in the understanding of NO pleiotropic effects in plant system, considering the last two decades of intensive research. Since NO biosynthesis remains unknown, a myriad of its down-stream effects was found to be affected by the cellular redox state. Therefore, the maintenance of the redox state in inoculated tissue appeared to have a pivotal role in the immune response establishment in potato.

P. infestans triggered NO burst in potato

Since NO burst is one of the first events observed after pathogen ingress, it is crucial to execute NO-dependent message to immune response in plants. At first, in the presented study we showed that potato leaves have had generated NO following inoculation with the avirulent race of *P. infestans*. In turn, the virulent race failed to initiate an early NO production. Primary NO overproduction was shown to be specific for the incompatibility of potato and the attacker. Many reports showed

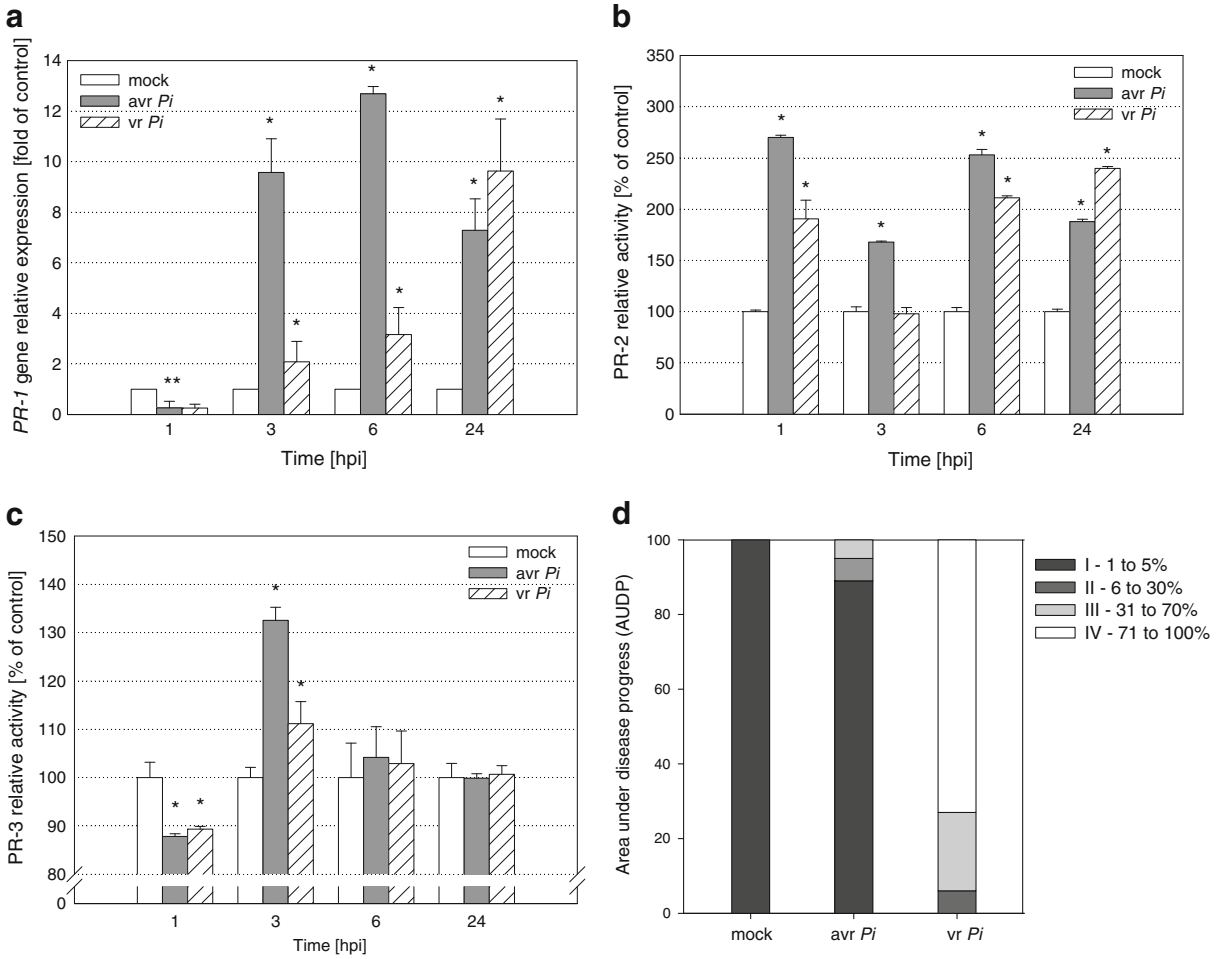

Fig. 4 The effect of *P. infestans* inoculation on potato leaves cv. 'Bzura': **a** time-course of *PR-1* gene expression upon inoculation using real-time RT-PCR semi-quantitative analysis, **b** relative activity of PR-2 protein (β-1,3-glucanase), **c** relative activity of PR-3 protein (chitinase), **d** index of disease development at 7 dpi, * significantly different from mock-inoculated potato leaves, $P<0.05$. Values represent the average of data±SD of at least three independent experiments

that NO action is dependent on its concentration and spatial production patterns (Besson-Bard et al. 2008; Kovacs and Lindermayr 2013). Others represented the standpoint that an early spatiotemporal NO burst is restricted to the incompatible interaction (Bennett et al. 2005; Mur et al. 2005). On this basis, we attempt to record NO-driven down-stream effects in both interactions. The attention was given to peroxynitrite and SNOs. A rapid formation of $ONOO^-$ as a result of the equimolar reaction of NO and $O_2^{\bullet-}$ in potato leaves treated with the avirulent race of pathogen indirectly indicated the activation of signaling towards resistance (Arasimowicz-Jelonek and Floryszak-Wieczorek 2011). However, Delledonne et al. (2001) documented that $ONOO^-$ is not a direct executor of HR in plants unlike in the animal system. It is worth noting that our previous findings revealed that in potato-*P. infestans* system oxidative burst has occurred since first hpi in both interactions. The difference between these responses has been observed afterwards, between 6 and 10 hpi (Floryszak-Wieczorek et al. 2011). The superoxide radical as the main component of oxidative burst may be produced in a controlled manner by plasma membrane NADPH oxidase (Noirot et al. 2014). In the presented study total NADPH oxidase activity was shown to be up-regulated since 1 hpi in *avr P. infestans*-treated leaves, what comprehensively correlated with the boosted $O_2^{\bullet-}$ accumulation. In turn, an increase in NADPH oxidase activity was weaker and occurred later in *vr P. infestans*-inoculated

leaves. Additionally, it needs to be emphasized that H_2O_2 accumulation governed by SOD activity increased greatly only in the incompatible interaction.

Obtained data are in line with previous findings that HR in soybean cells was activated after NO cooperation with H_2O_2 generated from $O_2^{\bullet-}$ by superoxide dismutase (De Stefano et al. 2006). These results revealed that in tobacco NO and H_2O_2 can act independently or in synergy and can share common components in regulating gene expression during defense responses in and outside the cell death program.

Collectively, these data highlighted the involvement of NO burst in the induction of redox changes in *avr P. infestans*-treated leaves. Further, the up-regulation of NADPH oxidase and the controlled $O_2^{\bullet-}$ production were tuned with SOD-mediated dismutation of $O_2^{\bullet-}$ to H_2O_2 triggering, in combination with NO, the cell death in potato inoculated leaves.

Redox re-adjustments determined resistance

Since an efficient immune response of potato leaves to *P. infestans* necessitates rapid changes in reactive nitrogen and oxygen species, an imbalance in redox homeostasis may occur as a result of these changes. To counteract oxidative stress, a spatiotemporally synchronized accumulation of non-enzymatic and enzymatic antioxidants must be employed (Groß et al. 2013). The cytoprotective effect of NO was reported to be linked to the NO-dependent regulation of the redox state and the controlling of ROS generation (Arasimowicz-Jelonek et al. 2014a, b). During the incompatible response of potato leaves an enhanced accumulation of ascorbate and total thiol content was observed early after pathogen recognition (1-6 hpi). This effect was triggered only in *avr P. infestans*-inoculated leaves, indicating fast and precisely controlled redox state re-adjustment. Markedly increased total antioxidative capacity recorded after inoculation with *avr P. infestans* was a symptom of the shifted redox potential to more reductive conditions. Interestingly, *Arabidopsis pad2-1* mutants, with an insufficient GSH supply, were unable to activate defense against the biotrophic *Phytophthora brassicae* or bacterial pathogen *Pseudomonas syringae* (Dubreuil-Maurizi et al. 2011). In turn, 6-phosphogluconolactonase 3 knock-down mutants of *Arabidopsis* (*pgl3*) with an enhanced *PRs* gene expression and a decreased redox potential possessed the constitutive activation of immune responses against *P. syringae* pv. *maculicola* and *Hyaloperonospora arabidopsidis* Noco2 (Xiong et al. 2009).

Summarizing, the ability of potato plants to control the redox state precisely under the pathogen pressure may modify the level of susceptibility/resistance to *P. infestans*. The implementation of redox re-adjustment processes was highly relevant to the type of interplay between potato and an oomycete pathogen. In fact, the antioxidative counteractions to redox imbalance impinged on the efficiency of defense expression in potato.

Nitric oxide-mediated S-nitrosylation

Considering NO bioactivity in plants, emphasis must be given to the storage of NO-coded message into the total SNO pool and S-nitrosylation of targeted proteins. The presence of NO-sensitive reactive Cys residues in low- and high-molecular mass molecules may serve as the molecular switch of NO functions in plants (Spadaro et al. 2010). Since particular Cys residues are sensitive to both the oxidative status of the cell and NO generation, they may combine two pathways that orchestrate early signaling, i.e. NO- and ROS-dependent (Yu et al. 2014). An augmented NO production in potato inoculated with the avirulent pathogen was tuned in time with a significant rise in the SNO pool (from 1 hpi). By contrast, no significant changes were noted in the compatible response. In proteins Cys may be a direct target of NO itself albeit NO may act indirectly via trans-nitrosylation reactions (Yu et al. 2014). Overall, the covalent attachment of NO to –SH groups of cysteine residues in protein and non-protein thiols may serve as a reversible redox-based modification, responsible for the execution of the NO-converted signal to a physiological response in plants (Spadaro et al. 2010). S-nitrosylation may modulate the activity of enzymes, the localization of proteins and the likelihood of interactions with other high-molecular mass molecules. Emerging evidence from particular studies indicate that an elevated SNO formation promoted plant resistance to a pathogen (Rustérucci et al. 2007). However, the accumulation of SNOs above a certain threshold may affect the SA-signaling pathway by a negative feedback loop, promoting NPR1 oligomerization in the cytoplasm and the suppression of defense (Malik et al. 2011). Therefore, SNO turnover controlled by an array of processes i.e. trans-nitrosylation reactions and enzymatic decomposition may be critical in the defense execution. Often, the

total SNO pool reflects the change of GSNO level – a mobile reservoir of NO bioactivity in plants. Discrepancies in GSNO content found in diverse pathosystem and GSNO localization must be kept in mind and may be a result of GSNOR distribution and different activity in plant cell compartments, tissues and organs (Corpas et al. 2013). For example, the tendency towards GSNO allocation in epidermal cells of sunflower plants was observed after inoculation with *avr Plasmopara halstedii* (Chaki et al. 2009). Emphasizing the role of denitrosylation processes, it must be stated that GSNOR is mainly involved in the breakdown of GSNO and currently limited information concerns other cellular specific SNO reductases or SNO lyases (Malik et al. 2011). Nevertheless, the excessive SNOs promoted the susceptibility of plants (Feechan et al. 2005). An emerging aspect of SNOs turn-over is the existence of specific forms of de-nitrosylation and the identification of cellular machinery to fine-tune SNOs pool.

It is generally accepted that changes in SNO contents, mediated by GSNO reductase, together with ROS governed by NADPH oxidase facilitated the immune promoting activity (Yun et al. 2011). However, in the presented study the postinfection GSNOR activity did not interfere entirely with the kinetics of SNO formation. The importance of GSNO reductase as a potato immune response controller was also highlighted in our previous reports concerning systemic acquired resistance and cross-tolerance of potato (Floryszak-Wieczorek et al. 2012; Janus et al. 2013; Arasimowicz-Jelonek et al. 2014a, b). As noted before, NO exported bioactivity was exhibited as an enhanced SNO storage at a relatively low threshold, governed temporarily by GSNOR activity.

One of the basic requirements of signal generation and transduction must be its transient character, enabling the reverse of signaling when it is required. Therefore, Cys residues may serve as an ideal substrate for targeted signaling since their NO-based modifications are mostly reversible and, as mentioned previously, exclusively redox-dependent (Spadaro et al. 2010).

Nitric oxide-mediated SNO formation influences rearrangements in the S-nitrosoproteome structure in physiological timelines and stress conditions (Fares et al. 2014). By performing the biotin-switch technique coupled with LC-MS/MS analysis, 104 proteins typed for S-nitrosylation were found in potato leaves at a decisive time-point after pathogen ingress (3 hpi). The presented list of potato S-nitrosylation targets (Table 1 Appendix) contains only *in vivo* S-nitrosylated proteins identified in mock and *P. infestans* challenge inoculated potato leaves. So far, a limited repertoire of functionally described S-nitrosylated proteins was uncovered in plants. Proteins subjected to S-nitrosylation presented in this study orchestrate an ample scope of cellular processes, including primary and secondary metabolism, redox maintenance and defense-related changes. Since available methods of SNOs identification in proteins are imperfect, we presented the supplemental list of potential S-nitrosylation targets in potato. Many among identified proteins are abundant in plant system and have been indicated as NO targets in different plant species. In the presented study, both CA and StSABP2 isoforms were found to be S-nitrosylation targets in potato challenged with *P. infestans*. It is worth noting that the attachment of NO to the cysteine residue of carbonic anhydrase was earlier recorded in GSNO-treated potato (Kato et al. 2013). Additionally, the role of CA in plant immunity is possibly linked to the lipid-base signaling and JA-responsive gene down-regulation (Hoang and Chapman 2002). These changes are believed to be profound in the relevant disease resistance development in plants. As documented before, the transfer of NO moiety to a specific Cys^{280} of AtSABP3 led to the inhibition of its carbonic anhydrase activity as well as blocked the ability of the protein to bind SA in an NO dose-dependent manner (Wang et al. 2008b). Both functions of AtSABP3 are essential in the establishment of *Arabidopsis* defense against virulent bacterial pathogens *Pst*DC3000, so that their inhibition by S-nitrosylation potentially contributed to the negative feedback loop, modulating SA-dependent plant immune responses. We would like to indicate that in potato exposed to *P. infestans*, thioredoxin M4 and 2-Cys peroxiredoxin – important players in the thioredoxin/thioredoxin reductase system, also undergo S-nitrosylation (Lindermayr et al. 2005; Romero-Puertas et al. 2007; Kato et al. 2013). In turn, superoxide dismutase as the following redox-related enzyme reported herein as S-nitrosylation target confirmed the findings of Kato et al. (2013). SOD activity has been believed to raise upon S-nitrosylation (Sehrawat et al. 2013) and that could potentially explain the up-regulation of SOD in the incompatible interaction of potato and *P. infestans*. So far, S-nitrosylation of SOD was presented in *Arabidopsis* (Lindermayr et al. 2005), *Kalanchoe pinnata* (Abat et al. 2008), citrus plants (Tanou et al. 2010) and potato (Kato et al. 2013). As well, the functional validation of

SOD S-nitrosylation was performed only in *Brassica juncea* (Sehrawat et al. 2013). Intriguingly, recently SOD has been reported to undergo inhibition by nitration of Tyr^{63} (Holzmeister et al. 2015).

From 104 presented S-nitrosylation candidates in the potato-*P. infestans* system, 17 were identified by us as nitration targets (unpublished data). The above mentioned list included e.g, two isoforms of carbonic anhydrase, chitinase, subtilisin-like protease-like, 2-Cys peroxiredoxin A, Rubisco small and large subunits, aldolase and chloroplast manganese stabilizing protein. This finding underpins the importance of dual protein regulation by Cys S-nitrosylation and Tyr residue nitration. It may serve as a basis of NO-based re-programming of the cell physiological status.

Hallmarks of potato defense

In our experimental approach, treatment of potato with *avr P. infestans* has activated *PR-1* and PR-2, the key indicators of plant defense against pathogens at the level of transcript accumulation and protein activity up-regulation, respectively. These findings are in line with previous reports concerning the compatible and incompatible interaction of plants and hemibiotrophic pathogens (Vleeshouwers et al. 2000; Wang et al. 2008a). Early up-regulation of the *PR-1* gene and β-1,3-glucanase were restricted only to the incompatible interaction. Activation of the *PR-1* gene depends on the signaling cascade often initiated by the NO burst and is orchestrated by salicylic acid bioactivity and redox state re-adjustments (Tada et al. 2008). As it was reported previously PR-2 activation at the transcript accumulation and protein activity level is likewise a part of potato defense against *P. infestans* (Arasimowicz-Jelonek et al. 2014a, b). However, the precise mode of action accompanying NO-mediated *PR* gene expression in potato is far from being resolved and needs further research. Nevertheless, PRs became fully operational at the early phase after inoculation. The delayed timing of *PR-1* expression (starting at 24 hpi) indicated insufficient defense activation against the virulent race of the pathogen. Wang et al. (2008a) demonstrated that a less virulent US-1 genotype of *P. infestans* caused the accumulation of the *PR-1*gene transcript earlier, from 8 hpi, in relation to the new more aggressive US-8 linage. Aggressive race induced the late gene up-regulation (at 48 hpi). In turn, only a slight increase of PR-3 activity in potato leaves was observed at 3 hpi, suggesting a less evident role of this enzyme in response to pathogens lacking chitin in cell walls. Consequently, in the light of presented findings, it may be concluded that mainly PR-1 and PR-2 effectively participated in the limiting of late blight disease.

Concluding remarks

The cross-talk of ROS- and RNS-based signaling is largely linked with redox-dependent modification on targeted cysteines in proteins, which may be considered as redox-switches of immune responses in potato leaves. So far, many protein targets were found to be subjected to S-nitrosylation, but still the precise mechanism is not fully understood and needs further research. Moreover, special emphasis must be given to perform a functional analysis of S-nitrosylated proteins engaged in non-model plant resistance, i.e. potato challenged by a pathogen. In consequence, the apprehension of NO fate is essential to warrant full understanding of NO influence on defense-orientated signaling in plants.

It is also true that currently we have no information as to whether and to what extent NO mediates *P. infestans* pathogenicity. Generally it is known that *P. infestans* is thought to accomplish colonization by molecular re-programing of the host defense strategy specifically by introducing an array of effectors (Vleeshouwers and Oliver 2014). According to Arasimowicz-Jelonek and Floryszak-Wieczorek (2014), the pathogen metabolic equipment to reset the NO signal and counteract nitrosative stress not only plays a role as a modulator of the host immune response, but might also be implicated in virulence. It is time to enrich our knowledge on *P. infestans* NO sensing and signaling, which may complete our understanding of pathogen-triggered re-programing of plant metabolism, moving elementarily the host-organism towards resistance or susceptibility.

Acknowledgments This study was funded from the National Science Centre (Preludium - grant number 2011/03/N/NZ9/00290). D. Abramowski would like to thank Dr. Christian Lindermayr, Institute of Biochemical Plant Pathology, Helmholtz Zentrum München, for advice in the biotin-switch assay.

Conflict of Interest The authors declare that they have no conflict of interest.

Appendixes

Table 1 The list of S-nitrosylation targets in potato leaves subjected to *P. infestans* inoculation

Band no.	Protein	Seq. identifier	Organism	Score	Mass	Function
1	Carbonic anhydrase[b,c,e,f]	22550386	*Solanum tuberosum*[a]	96	34811	Metabolic enzymes
2	ferredoxin-dependent glutamate synthase 1, chloroplastic/mitochondrial-like[f]	565396313	*Solanum tuberosum*[a]	333	178149	Metabolic enzymes
2	photosystem II 47 kDa protein	11465984	*Nicotiana tabacum,*	223	56117	Photosynthesis-involved proteins
2	phosphoglycerate kinase precursor[b]	3328122	*Solanum tuberosum*	126	50561	Metabolic enzymes
2	germin-like protein 1[g,h]	4239821	*Oryza sativa*	88	21984	Others
2	protease inhibitor/seed storage/lipid transfer protein family protein[c]	317411422	*Brassica rapa subsp. pekinensis*	72	18590	Others
2	chlorophyll A/B binding protein 8	543176847	*Phaseolus vulgaris, Solanum tuberosum*[a]	75	29719	Photosynthesis-involved proteins
2	ADP/ATP translocator	350540644	*Solanum lycopersicum, Solanum tuberosum*[a]	70	42124	Metabolic enzymes
2	photosystem I subunit X Precursor	565393696	*Arabidopsis thaliana, Solanum tuberosum*[a]	66	13357	Photosynthesis-involved proteins
2	polyubiquitin	21608	*Solanum tuberosum*	58	1693	Others
2	33 kDa precursor protein of oxygen-evolving complex[d,e,i]	809113	*Solanum tuberosum*	52	35420	Metabolic enzymes
3	mechanosensitive ion channel protein 3, chloroplastic-like isoform X1	502133071	*Cicer arietinum*	54	65302	Others
3	ribulose-1,5-bisphosphate carboxylase/oxygenase small subunit[c,d,e,i]	162946537	*Solanum tuberosum*	68	20803	Photosynthesis-involved proteins
4	Chlorophyll a-b binding protein 36, chloroplastic	413968458	*Solanum tuberosum*	140	29617	Photosynthesis-involved proteins
4	putative glycine-rich RNA binding protein 1[b]	6911142	*Catharanthus roseus*	66	13811	Others
4	exportin1 family protein	566234718	*Populus trichocarpa*	57	125104	Metabolic enzymes
4	Photosystem Q(B) protein / Photosystem II D1 protein	940008	*Solanum nigrum,Solanum tuberosum*[a]	108	38953	Photosynthesis-involved proteins
5	leucine-rich repeat transmembrane protein kinase-like protein	15226197	*Arabidopsis thaliana*	68	79086	Others
5	putative LZ-NBS-LRR resistance protein	73658558	*Rosa hybrid cultivar*	54	24274	Defense-related proteins
5	transketolase[e,f]	568214657	*Solanum tuberosum*	396	80264	Metabolic enzymes
5	leaf rust resistance protein Lr10	305691103	*Triticum dicoccoides*	57	105901	Defense-related proteins
5	subtilisin-like protease SDD1-like[f]	565396156	*Solanum tuberosum*[a]	118	79519	Redox-related proteins
5	methionine synthase	568215268	*Solanum tuberosum*	85	24614	

Table 1 (continued)

Band no.	Protein	Seq. identifier	Organism	Score	Mass	Function
						Metabolic enzymes
5	hydroxyproline-rich glycoprotein homolog	2244847	*Arabidopsis thaliana*	55	56463	Others
5	kinesin-like calmodulin-binding protein-like	460374958	*Solanum lycopersicum*	52	143938	Others
5	putative chromatin remodeling protein SYD	13603721	*Arabidopsis thaliana*	52	391293	Others
6	Heat shock 70 kDa protein[e]	565348852	*Solanum tuberosu*[a]	116	72165	Metabolic enzymes
6	Elongation factor 1-alpha[b,d,g]	24745945	*Solanum tuberosum*	100	49503	Metabolic enzymes
6	beta-xylosidase/alpha-L-arabinofuranosidase 2-like[f]	565370398	*Solanum tuberosum*[a]	87	86056	Metabolic enzymes
6	alpha tubulin[f]	11967906	*Nicotiana tabacumN Solanum tuberosum*[a]	69	50277	Metabolic enzymes
6	pre-mRNA-splicing factor ATP-dependent RNA helicase PRP16-like	449462491	*Cucumis sativus*	61	146920	Others
7	photosystem I P700 apoprotein A1	82754627	*Solanum tuberosum*	113	8321	Photosynthesis-involved proteins
7	F precursor DLD	568215578	*Solanum tuberosum*	56	53603	Metabolic enzymes
8	fasciclin-like arabinogalactan protein 10-like FLA10[c]	565344709	*Solanum tuberosum*[a]	55	43405	Metabolic enzymes
8	ribulose-1,5-bisphosphate carboxylase/oxygenase large subunit[b,c,d,e,g]	108773138	*Solanum tuberosum*	891	53279	Photosynthesis-involved proteins
8	ATP synthase CF1 alpha chain[b,d,j]	82754614	*Solanum tuberosum*	1995	55389	Metabolic enzymes
8	ATP synthase CF1 beta subunit[c]	108773137	*Solanum tuberosum*	1499	53521	Metabolic enzymes
8	9-cis-epoxycarotenoid dioxygenase NCED6, chloroplastic-like	565365668	*Solanum tuberosum*[a]	65	65575	Redox-related proteins
9	wall-associated receptor kinase 4-like	357155195	*Brachypodium distachyon*	72	102087	Others
9	triose phosphate/phosphate translocator, chloroplastic precursor	568214794	*Solanum tuberosum*	68	43907	Photosynthesis-involved proteins
9	F-box/LRR-repeat protein 7-like	449489483	*Cucumis sativus*[a]	63	52521	Others
9	fatty acid hydroperoxide lyase HPL	14627128	*Solanum tuberosum*	162	54272	Redox-related proteins
9	glutamate–glyoxylate aminotransferase 2-like	565382582	*Solanum tuberosum*[a]	143	53813	Metabolic enzymes
9	hydroperoxide lyase	4850214	*Solanum lycoperiscum*	109	54116	Redox-related proteins
9	UTP–glucose-1-phosphate uridylyltransferase[b]	21599	*Solanum tuberosum*	60	51982	Metabolic enzymes
10	leucine aminopeptidase, chloroplastic-like[c]	565366865	*Solanum tuberosum*[a]	390	60666	Metabolic enzymes
10	serine–glyoxylate aminotransferase-like	565366189	*Solanum tuberosum*[a]	132	44179	Metabolic enzymes

Table 1 (continued)

Band no.	Protein	Seq. identifier	Organism	Score	Mass	Function
10	adenylosuccinate synthetase, chloroplastic-like	565369405	*Solanum tuberosum*[a]	68	55768	Metabolic enzymes
10	2,3-dimethylmalate lyase-like / carboxyvinyl-carboxyphosphonate phosphorylmutase, chloroplastic-like	460387983	*Solanum tuberosum*[a]	66	54716	Metabolic enzymes
11	phosphoglycerate kinase, chloroplastic-like[e]	568214597	*Solanum tuberosum*	301	50601	Metabolic enzymes
11	photosystem II CP43 protein	149208886	*Phragmites australis*	413	45973	Photosynthesis-involved proteins
11	peroxisomal (S)-2-hydroxy-acid oxidase GLO1-like isoform X1	565363307	*Solanum tuberosum*[a]	595	40631	Metabolic enzymes
11	glycerate dehydrogenase HPR, peroxisomal	565387855	*Solanum tuberosum*[a]	314	42462	Metabolic enzymes
11	glycerate dehydrogenase isoform 1 / NADH-dependent hydroxypyruvate reductase	508705745	*Theobroma cacao*	292	42467	Photosynthesis-involved proteins
11	phosphoribulokinase, chloroplastic-like	565372690	*Solanum tuberosum*[a]	165	45160	Photosynthesis-involved proteins
11	mRNA binding protein precursor / chloroplast stem-loop binding protein of 41 kDa a, chloroplastic-like[f]	565365980	*Solanum tuberosum*	114	43366	Photosynthesis-involved proteins
11	peptidyl-prolyl cis-trans isomerase, chloroplastic-like	460372959	*Solanum tuberosum*[a]	92	49486	Metabolic enzymes
11	NADH dehydrogenase subunit 7	108773185	*Solanum tuberosum*	84	45699	Metabolic enzymes
11	NAD-dependent epimerase/dehydratase family protein-like protein	568214776	*Solanum tuberosum*[a]	73	42751	Metabolic enzymes
11	aspartate aminotransferase, chloroplastic-like	568215485	*Solanum tuberosum*	66	51652	Metabolic enzymes
11	thioredoxin M4, chloroplastic-like[b]	565386346	*Solanum tuberosum*[a]	65	19512	Redox-related proteins
11	homeobox-leucine zipper protein GLABRA 2-like	449519629	*Cucumis sativus*	61	82824	Others
11	phospholipase A1-IIgamma-like DSEL	565397487	*Solanum tuberosum*[a]	58	45012	Metabolic enzymes
11	transposase	334902911	*Solanum demissum*	56	125694	Others
12	glyceraldehyde-3-phosphate dehydrogenase[b,e,f]	22094840	*Solanum tuberosum*	103	36762	Metabolic enzymes
12	fructose-bisphosphate aldolase, cytoplasmic isozyme 1[c,e,f]	565358575	*Solanum tuberosum*[a]	208	38423	Photosynthesis-involved proteins
12	putative mitochondrial NAD-dependent malate dehydrogenase[c,f,h]	21388544	*Solanum tuberosum*	226	35823	Metabolic enzymes
12	photosystem I reaction center subunit XI, chloroplastic-like	565402715	*Solanum tuberosum*[a]	71	23220	Photosynthesis-involved proteins
12	chloroplast sedoheptulose-1,7-bisphosphatase[e]	565378420	*Solanum tuberosum*	242	42928	Photosynthesis-involved proteins

Table 1 (continued)

Band no.	Protein	Seq. identifier	Organism	Score	Mass	Function
12	coproporphyrinogen-III oxidase, chloroplastic-like	565372070	*Solanum tuberosum*[a]	129	45613	Metabolic enzymes
12	2-Cys peroxiredoxin A (previously known as BAS1-like, chloroplastic-like)[b,c,f,k]	21912927	*Solanum tuberosum*[a]	121	30048	Redox-related proteins
12	porphobilinogen deaminase, chloroplastic-like	565358446	*Solanum tuberosum*[a]	117	39498	Metabolic enzymes
12	quinone oxidoreductase-like protein, chloroplastic-like	565399387	*Solanum tuberosum*[a]	68	41008	Redox-related proteins
13	ATP synthase gamma chain, chloroplastic-like	565362769	*Solanum tuberosum*[a]	191	41568	Metabolic enzymes
13	class I chitinase[c,f]	6707113	*Solanum tuberosum*	108	36136	Defense-related proteins
13	class I chitinase precursor[c]	568214310	*Solanum tuberosum*	87	36224	Defense-related proteins
13	noyl-[acyl-carrier-protein] reductase [NADH], chloroplastic-like	565375369	*Solanum tuberosum*[a]	82	41960	Metabolic enzymes
13	ferredoxin–NADP reductase, leaf-type isozyme, chloroplastic-like	565347451	*Solanum tuberosum*[a]	590	40661	Metabolic enzymes
14	chloroplast manganese stabilizing protein[c]	313586398	*Solanum tuberosum*	151	34280	Photosynthesis-involved proteins
14	cytochrome f	91209001	*Solanum bulbocastanum*	148	35288	Metabolic enzymes
14	extracellular Ca^{2+} sensing receptor	565356427	*Solanum tuberosum*[a]	71	42445	Others
14	Endochitinase 2; precursor	1705808	*Solanum tuberosum*	100	34389	Defense-related proteins
15	chloroplast manganese stabilizing protein-II	239911810	*Solanum tuberosum*	397	31398	Photosynthesis-involved proteins
15	harpin binding protein 1	568215184	*Solanum tuberosum*	137	30257	Others
15	photosystem II D2 protein	91208983	*Solanum bulbocastanum*	376	39694	Photosynthesis-involved proteins
15	chlorophyll a-b binding protein CP29.1, chloroplastic-like	565401730	*Solanum tuberosum*[a]	210	31157	Photosynthesis-involved proteins
15	phosphoglycolate phosphatase 1B, chloroplastic-like	565373406	*Solanum tuberosum*[a]	135	39891	Metabolic enzymes
15	cytochrome f	91209001	*Solanum bulbocastanum*	131	35288	Metabolic enzymes
15	auxin-induced in root cultures protein 12-like	2894118	*Solanum tuberosum*[a]	89	16445	Others
15	superoxide dismutase [Fe] 2, chloroplastic-like isoform X1[b,d,e,g]	565384504	*Solanum tuberosum*[a]	70	34775	Redox-related proteins
15	superoxide dismutase [Fe] 2, chloroplastic-like isoform X2[b,d,e,g]	565384508	*Solanum tuberosum*[a]	70	34519	Redox-related proteins
16	carbonic anhydrase, chloroplastic-like isoform X1[b,c]	565342863	*Solanum tuberosum*[a]	111	36291	Metabolic enzymes
16	carbonic anhydrase, chloroplastic-like isoform X2[b,c]	565342865	*Solanum tuberosum*[a]	111	34842	Metabolic enzymes

Table 1 (continued)

Band no.	Protein	Seq. identifier	Organism	Score	Mass	Function
16	salicylic acid-binding protein 2	565390197	*Solanum tuberosum*[a]	94	16493	Defense-related proteins
16	Rubber elongation factor protein	132270	*Hevea brasiliensis*	161	14713	Others
16	chlorophyll a-b binding protein CP26, chloroplastic-like[f]	565382242	*Solanum tuberosum*[a]	401	30438	Photosynthesis-involved proteins
16	chlorophyll a-b binding protein 3C-like[b]	413968456	*Solanum tuberosum*	247	25059	Photosynthesis-involved proteins
16	triosephosphate isomerase cytosolic isoform[b,,e,f]	565400366	*Solanum tuberosum*[a]	193	27195	Metabolic enzymes
16	triosephosphate isomerase, chloroplastic-like	565403781	*Solanum tuberosum*[a]	174	34208	Metabolic enzymes
17	Photosystem I reaction center subunit II, chloroplastic	565380579	*Solanum tuberosum*[a]	379	22838	Photosynthesis-involved proteins
17	putative Rieske Fe-S protein precursor[d]	413968462	*Solanum tuberosum*	58	24591	Others
18	cytochrome b6-f complex iron-sulfur subunit, chloroplastic	568214334	*Solanum tuberosum*	173	24527	Metabolic enzymes
18	aspartic proteinase inhibitor / Kunitz-type protease inhibitor precursor[b,c]	20386375	*Solanum tuberosum*	100	24339	Metabolic enzymes
18	cytochrome b6/f complex subunit IV	91209018	*Solanum bulbocastanum*	91	17507	Metabolic enzymes
18	nucleoside diphosphate kinase 2, chloroplastic-like	565361307	*Solanum tuberosum*[a]	91	24875	Others
18	peptidylprolyl isomerase	210062274	*Solanum tuberosum*[a]	76	27870	Metabolic enzymes

[a] Predicted sequence

[b] Reported earlier as S-nitrosylated in potato (Kato et al. 2013)

[c] Nitrated in potato (data unpublished)

[d] Identified by Lindermayr et al. 2005

[e] Identified by Abat et al. 2008

[f] Identified by Vanzo et al. 2014

[g] By Fares et al. 2011

[h] By Tanou et al. 2009

[h] Romero-Puertas et al. 2007

[i] Ortega-Galisteo et al. 2012

[j] Palmieri et al. 2010

[k] Wang et al. 2008b

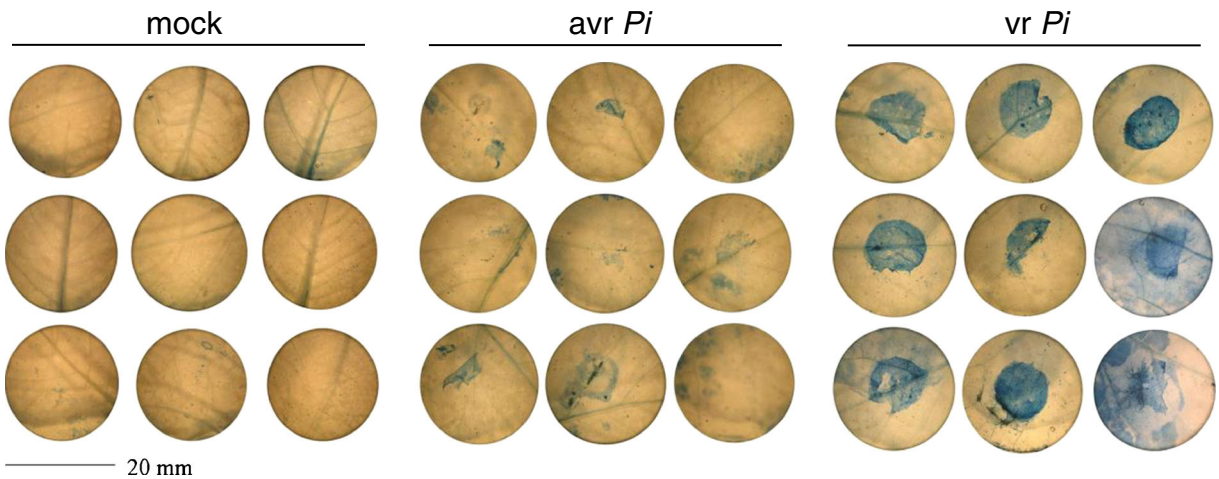

Fig. 5 Late blight disease progress in potato leaves-excised discs inoculated with *avr* and *vr P. infestans*. Average area of *P. infestans* mycelium growth was 2.98±0.17 % in *avr P. infestans*-treated potato; and 20.1±1.6 % in *vr P. infestans*-treated potato. Values represent the average of data±SD of six independent experiments with maintained randomization

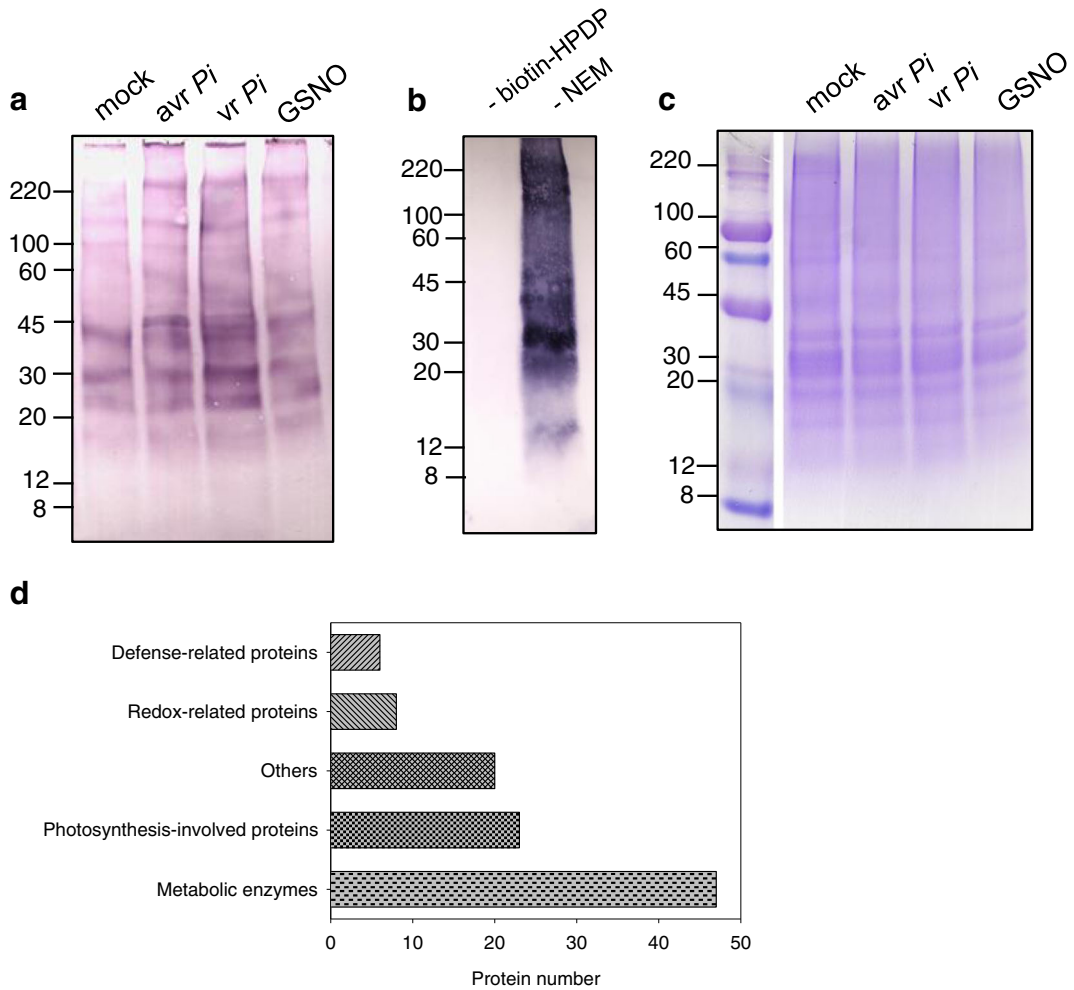

Fig. 6 Identification of S-nitrosylation targets in potato leaves: **a** immunodetection of S-nitrosylated proteins with the indication of the bands subjected to densytometric analysis, **b** negative and positive controls in BST, **c** protein content visualization using Coomassie blue staining, **d** functional categorization of the 104 identified S-nitrosylated proteins in potato leaves

References

Abat, J. K., Mattoo, A. K., & Deswal, R. (2008). S-nitrosylated proteins of a medicinal CAM plant *Kalanchoe pinnata*-ribulose-1,5-bisphosphate carboxylase/oxygenase activity targeted for inhibition. *FEBS Journal, 275*, 2862–2872.

Abeles, F., & Forrence, L. (1970). Temporal and Hormonal Control of β-1,3-Glucanase in *Phaseolus vulgaris* L. *Plant Physiology, 45*, 395–400.

Able, A. J., Guest, D. I., & Sutherland, M. W. (1998). Use of a new tetrazolium-based assay to study the production of superoxide radicals by tobacco cell cultures challenged with avirulent zoospores of *Phytophthora parasitica* var *nicotianae. Plant Physiology, 117*, 491–499.

Arasimowicz-Jelonek, M., & Floryszak-Wieczorek, J. (2011). Understanding the fate of peroxynitrite in plant cells–from physiology to pathophysiology. *Phytochemistry, 72*, 681–688.

Arasimowicz-Jelonek, M., & Floryszak-Wieczorek, J. (2014). Nitric oxide: an effective weapon of the plant or the pathogen? *Molecular Plant Patholology, 15*(4), 406–416.

Arasimowicz-Jelonek, M., Floryszak-Wieczorek, J., Drzewiecka, K., Chmielowska-Bąk, J., Abramowski, D., & Izbiańska, K. (2014a). Aluminum induces cross-resistance of potato to *Phytophthora infestans. Planta, 239*, 679–694.

Arasimowicz-Jelonek, M., Floryszak-Wieczorek, J., Abramowski, D., Izbiańska, K. (2014b) Nitric oxide and reactive nitrogen species. In: nitric oxide in plants: metabolism and role ins tress physiology. Springer International Publishing, pp 165–184.

Astier, J., Rasul, S., Koen, E., Manzoor, H., Besson-Bard, A., Lamotte, O., Jeandroz, S., Durner, J., Lindermayr, C., & Wendehenne, D. (2011). S-nitrosylation: an emerging post-

translational protein modification in plants. *Plant Science: An International Journal of Experimental Plant Biology, 181*, 527–533.

Barroso, J. B., Corpas, F. J., Carreras, A., Rodríguez-Serrano, M., Esteban, F. J., Fernández-Ocaña, A., Chaki, M., Romero-Puertas, M. C., Valderrama, R., Sandalio, L. M., & del Río, L. A. (2006). Localization of S-nitrosoglutathione and expression of S-nitrosoglutathione reductase in pea plants under cadmium stress. *Journal of Experimental Botany, 57*, 1785–1793.

Beauchamp, C., & Fridovich, I. (1971). Superoxide dismutase: improved assays and an assay applicable to acrylamide gels. *Analytical Biochemistry, 44*, 276–287.

Becana, M., Aparicio-Tejo, P., Irigoyen, J. J., & Sanchez-Diaz, M. (1986). Some enzymes of hydrogen peroxide metabolism in leaves and root nodules of *Medicago sativa*. *Plant Physiology, 82*, 1169–1171.

Bennett, M., Mehta, M., & Grant, M. (2005). Biophoton imaging: a nondestructive method for assaying R gene responses. *Molecular Plant-Microbe Interactions, 18*, 95–102.

Besson-Bard, A., Griveau, S., Bedioui, F., & Wendehenne, D. (2008). Real-time electrochemical detection of extracellular nitric oxide in tobacco cells exposed to cryptogein, an elicitor of defence responses. *Journal of Experimental Botany, 59*, 3407–3414.

Chaki M., Lindermayr C. (2014) S-Nitrosoglutathione Reductase: Key Regulator of Plant Development and Stress Response. In: Khan MN, Mobin M, Mohammad F, Corpas FJ (eds) Nitric oxide in plants: metabolism and role in stress physiology. Springer International Publishing, pp 139–151.

Chaki, M., Fernández-Ocaña, A. M., Valderrama, R., Carreras, A., Esteban, F. J., Luque, F., Gómez-Rodrígez, M. V., Begara-Morales, J. C., Corpas, F. J., & Barroso, J. B. (2009). Involvement of reactive nitrogen and oxygen species (RNS and ROS) in sunflower-mildew interaction. *Plant and Cell Physiology, 50*, 265–279.

Chomcznski, P., & Sacchi, N. (1987). Single-step method of RNA isolation by acid quanidinium thiocyanate-phenol-chloroform extraction. *Analytical Biochemistry, 162*, 156.

Corpas, F. J., Palma, J. M., Del Río, L. A., & Barroso, J. B. (2013). Protein tyrosine nitration in higher plants grown under natural and stress conditions. *Frontiers in Plant Science, 4*, 29.

Delledonne, M., Xia, Y., Dixon, R. A., & Lamb, C. (1998). Nitric oxide functions as a signal in plant disease resistance. *Nature, 394*, 585–588.

Delledonne, M., Zeier, J., Marocco, A., & Lamb, C. (2001). Signal interactions between nitric oxide and reactive oxygen intermediates in the plant hypersensitive disease resistance response. *Proceedings of the National Academy of Sciences, 98*, 13454–13459.

Doke, N. (1983). Involvement of superoxide anion generation in the hypersensitive response of potato tuber tissues to infection with an incompatible race of *Phytophthora infestans* and to the hyphal wall components. *Physiologial Plant Pathology, 23*, 345–357.

Dubreuil-Maurizi, C., Vitecek, J., Marty, L., Branciard, L., Frettinger, P., Wendehenne, D., Meyer, A. J., Mauch, F., & Poinssot, B. (2011). Glutathione deficiency of the *Arabidopsis* mutant *pad2-1* affects oxidative stress-related events, defense gene expression, and the hypersensitive response. *Plant Physiology, 157*, 2000–2012.

Fares, A., Rossignol, M., & Peltier, J. B. (2011). Proteomics investigation of endogenous S-nitrosylation in Arabidopsis. *Biochemical and Biophysical Research Communications, 416*(3-4), 331–336.

Fares, A., Nespoulous, C., Rossignol, M., & Peltier, J.-B. (2014). Simultaneous identification and quantification of nitrosylation sites by combination of biotin switch and ICAT labeling. *Methods in Molecular Biology, 1072*, 609–620.

Feechan, A., Kwon, E., Yun, B.-W., Wang, Y., Pallas, J. A., & Loake, G. J. (2005). A central role for *S*-nitrosothiols in plant disease resistance. *Proceedings of the National Academy of Sciences of the United States of America, 102*(22), 8054–8059.

Floryszak-Wieczorek, J., Górski, W., & Arasimowczi-Jelonek, M. (2011). Functional imaging of biophoton responses of plants to fungal infection. *European Journal of Plant Pathology, 130*, 249–258.

Floryszak-Wieczorek, J., Arasimowicz-Jelonek, M., Milczarek, G., Janus, L., Pawlak-Sprada, S., Abramowski, D., Deckert, J., & Billert, H. (2012). Nitric oxide–mediated stress imprint in potato as an effect of exposure to a priming agent. *Molecular Plant-Microbe Interactions, 25*, 1469–1477.

Floryszak-Wieczorek J., Arasimowicz-Jelonek M., Abramowski D. (2013) Redox-sensing responses in the potato-*Phtophthora infestans* system. Oxidative stress and cell death in plants: mechanisms and implications Florence, Italy, p. 53.

Groß, F., Durner, J., & Gaupels, F. (2013). Nitric oxide, antioxidants and prooxidants in plant defence responses. *Frontiers in Plant Science, 4*, 419.

Hoang, C. V., & Chapman, K. D. (2002). Biochemical and molecular inhibition of plastidial carbonic anhydrase reduces the incorporation of acetate into lipids in cotton embryos and tobacco cell suspensions and leaves. *Plant Physiology, 128*, 1417–1427.

Holzmeister, C., Gaupels, F., Geerlof, A., Sarioglu, H., Sattler, M., Durner, J., & Lindermayr, C. (2015). Differential inhibition of *Arabidopsis* superoxide dismutases by peroxynitrite-mediated tyrosine nitration. *Journal of Experimental Botany, 66*(3), 989–999.

Huang, J., Li, D., Diao, J., Hou, J., Yuan, J., & Zou, G. (2007). A novel fluorescent method for determination of peroxynitrite using folic acid as a probe. *Talanta, 72*, 1283–1287.

James, W. C. (1971). An illustrated series of assessment keys for plant diseases, their preparation and usage. *Canadian Plant Disease Survey, 51*, 39–65.

Janus, Ł., Milczarek, G., Arasimowicz-Jelonek, M., Abramowski, D., Billert, H., & Floryszak-Wieczorek, J. (2013). Normoergic NO-dependent changes, triggered by a SAR inducer in potato, create more potent defense responses to *Phytophthora infestans*. *Plant Science, 211*, 23–34.

Kato, H., Takemoto, D., & Kawakita, K. (2013). Proteomic analysis of S-nitrosylated proteins in potato plant. *Physiologia Plantarum, 148*, 371–386.

Kovacs, I., & Lindermayr, C. (2013). Nitric oxide-based protein modification: formation and site-specificity of protein S-nitrosylation. *Frontiers in Plant Science, 4*, 137.

Lim, M. H., Xu, D., & Lippard, S. J. (2006). Visualization of nitric oxide in living cells by a copper-based fluorescent probe. *Nature Chemical Biology, 2*, 375–380.

Lindermayr, C., Saalbach, G., & Durner, J. (2005). Proteomic Identification of S-Nitrosylated Proteins in *Arabidopsis*. *Plant Physiology, 137*, 921–930.

Malik, S. I., Hussain, A., Yun, B.-W., Spoel, S. H., & Loake, G. J. (2011). GSNOR-mediated de-nitrosylation in the plant defence response. *Plant Science, 181*, 540–544.

Mukherjee, S. P., & Choudhuri, M. A. (1983). Implications of water stress-induced changes in the levels of endogenous ascorbic acid and hydrogen peroxide in *Vigna* seedlings. *Physiologia Plantarum, 58*, 166–170.

Mur, L. A. J., Santosa, I. E., Laarhoven, L. J. J., Holton, N. J., Harren, F. J. M., & Smith, A. R. (2005). Laser photoacoustic detection allows in planta detection of nitric oxide in tobacco following challenge with avirulent and virulent *Pseudomonas syringae* Pathovars. *Plant Physiology, 138*, 1247–1258.

Noctor, G., Mhamdi, A., Chaouch, S., Han, Y., Neukermans, J., Marquez-Garcia, B., Queval, G., & Foyer, C. H. (2012). Glutathione in plants: an integrated overview. *Plant, Cell & Environment, 35*, 454–484.

Noirot, E., Der, C., Lherminier, J., Robert, F., Moricova, P., Kieu, K., Leborgne-Castel, N., Simon-Plas, F., & Bouhidel, K. (2014). Dynamic changes in the subcellular distribution of the tobacco ROS-producing enzyme RBOHD in response to the oomycete elicitor cryptogein. *Journal of Experimental Botany, 65*, 5011–5022.

Noritake, T., Kawakita, K., & Doke, N. (1996). Nitric oxide induces phytoalexin accumulation in potato tuber tissues. *Plant Cell Physiology, 37*, 113–116.

Ortega-Galisteo, A. P., Rodriguez-Serrano, M., Pazmino, D. M., Gupta, D. K., Sandalio, L. M., & Romero-Puertas, M. C. (2012). S-Nitrosylated proteins in pea (*Pisum sativum* L.) leaf peroxisomes: changes under abiotic stress. *Journal of Experimental Botany, 63*, 2089–2103.

Palmieri, M. C., Lindermayr, C., Bauwe, H., Steinhauser, C., & Durner, J. (2010). Regulation of plant glycine decarboxylase by s-nitrosylation and glutathionylation. *Plant Physiology, 152*(3), 1514–1528.

Pauly, M., Andersen, L. N., Kauppinen, S., Kofod, L. V., York, W. S., Albersheim, P., & Darvill, A. (1999). A xyloglucan-specific endo-beta-1,4-glucanase from *Aspergillus aculeatus*: expression cloning in yeast, purification and characterization of the recombinant enzyme. *Glycobiology, 9*, 93–100.

Pfaffl, M. W. (2001). A new mathematical model for relative quantification in real-time RT-PCR. *Nucleic Acids Research, 29*, 2004–2007.

Re, R., Pellegrini, N., Proteggente, A., Pannala, A., Yang, M., & Rice-Evans, C. (1999). Antioxidant activity applying an improved ABTS radical cation decolorization assay. *Free Radical Biology & Medicine, 26*, 1231–1237.

Rice-Evans, C. A., Diplock, A. T., & Symons, M. C. R. (1991). Techniques in free radical research. *Laboratory Techniques in Biochemistry and Molecular Biology, 22*, 143–147.

Romero-Puertas, M. C., Laxa, M., Matte, A., Zaninotto, F., Finkemeier, I., Jones, A. M. E., Perazzolli, M., Vandelle, E., Dietz, K.-J., & Delledonne, M. (2007). S-Nitrosylation of peroxiredoxin ii e promotes peroxynitrite-mediated tyrosine nitration. *The Plant Cell, 19*, 4120–4130.

Rustérucci, C., Espunya, M. C., Díaz, M., Chabannes, M., & Martínez, M. C. (2007). S-Nitrosoglutathione reductase affords protection against pathogens in *Arabidopsis*, both locally and systemically. *Plant Physiology, 143*, 1282–1292.

Sehrawat A., Abat J.K., Deswal R. (2013) RuBisCO depletion improved proteome coverage of cold responsive S-nitrosylated targets in *Brassica juncea*. Frontiers in Plant Science, 4, doi:10.3389/fpls.2013.00342.

Spadaro, D., Yun, B.-W., Spoel, S. H., Chu, C., Wang, Y.-Q., & Loake, G. J. (2010). The redox switch: dynamic regulation of protein function by cysteine modifications. *Physiologia Plantarum, 138*, 360–371.

Stefano, M., Vandelle, E., Polverari, A., Ferrarini, A., & Delledonne, M. (2006). Nitric oxide-mediated signaling functions during the plant hypersensitive response. In L. Lamattina & J. C. Polacco (Eds.), *Nitric oxide in plant growth* (pp. 207–222). Berlin, Heidelberg: Development and Stress Physiology. Springer Berlin Heidelberg.

Tada, Y., Spoel, S. H., Pajerowska-Mukhtar, K., Mou, Z., Song, J., Wang, C., Zuo, J., & Dong, X. (2008). Plant immunity requires conformational changes of NPR1 via S-nitrosylation and thioredoxins. *Science, 321*, 952–956.

Tanou, G., Job, C., Rajjou, L., Arc, E., Belghazi, M., Diamantidis, G., Molassiotis, A., & Job, D. (2009). Proteomics reveals the overlapping roles of hydrogen peroxide and nitric oxide in the acclimation of citrus plants to salinity. *Plant Journal, 60*(5), 795–804.

Tanou, G., Job, C., Belghazi, M., Molassiotis, A., Diamantidis, G., & Job, D. (2010). Proteomic signatures uncover hydrogen peroxide and nitric oxide cross-talk signaling network in citrus plants. *Journal of Proteome Research, 2010*(11), 5994–6006.

Vanzo, E., Ghirardo, A., Merl-Pham, J., Lindermayr, C., Heller, W., Hauck, S. M., Durner, J., & Schnitzler, J.-P. (2014). S-Nitroso-proteome in poplar leaves in response to acute ozone stress. *PLoS ONE, 9*(9), e106886. doi:10.1371/journal.pone.0106886.

Vleeshouwers, V. G. A. A., & Oliver, R. P. (2014). Effectors as tools in disease resistance breeding against biotrophic, hemibiotrophic, and necrotrophic plant pathogens. *Molecular Plant-Microbe Interactions, 27*, 196–206.

Vleeshouwers, V. G., van Dooijeweert, W., Govers, F., Kamoun, S., & Colon, L. T. (2000). The hypersensitive response is assiociated with host and non-host resistance to *Phytophthora infestans*. *Planta, 210*, 853–864.

Wang, X., El Hadrami, A., Adam, L. R., & Daayf, F. (2008a). Differential activation and suppression of potato defence responses by *Phytophthora infestans* isolates representing US-1 and US-8 genotypes. *Plant Pathology, 57*, 1026–1037.

Wang, Y.-Q., Feechan, A., Yun, B.-W., Shafiei, R., Hofmann, A., Taylor, P., Xue, P., Yang, F.-Q., Xie, Z.-S., Pallas, J. A., Chu, C.-C., & Loake, G. J. (2008b). S-Nitrosylation of AtSABP3 antagonizes the expression of plant immunity. *Journal of Biological Chemistry, 284*, 2131–2137.

Wilson, U. E., Coffey M. D. (1980). Cytological evaluation of general resistance to Phytophthora infestans in potato foliage. *Annals of Botany, 45*, 81–90.

Xiong, Y., DeFraia, C., Williams, D., Zhang, X., & Mou, Z. (2009). Characterization of *Arabidopsis* 6-phosphogluconolactonase T-DNA insertion mutants reveals an essential role for the oxidative section of the plastidic pentose phosphate pathway in plant growth and development. *Plant & Cell Physiology, 50*, 1277–1291.

Ye, J., Coulouris, G., Zaretskaya, I., Cutcutache, I., Rozen, S., & Madden, T. L. (2012). Primer-BLAST: a tool to design target-specific primers for polymerase chain reaction. *BMC Bioinformatics, 13*, 134.

Yu, M., Lamattina, L., Spoel, S. H., & Loake, G. J. (2014). Nitric oxide function in plant biology: a redox cue in deconvolution. *New Phytologist, 202*, 1142–1156.

Yun, B.-W., Feechan, A., Yin, M., Saidi, N. B. B., Le Bihan, T., Yu, M., Moore, J. W., Kang, J.-G., Kwon, E., Spoel, S. H., Pallas, J. A., & Loake, G. J. (2011). S-nitrosylation of NADPH oxidase regulates cell death in plant immunity. *Nature, 478*, 264–268.

Zhao, S., & Fernald, R. D. (2005). Comprehensive algorithm for quantitative real-time polymerase chain reaction. *Journal of Computational Biology, 12*, 1047–1064.